

RSC Advances



This is an *Accepted Manuscript*, which has been through the Royal Society of Chemistry peer review process and has been accepted for publication.

Accepted Manuscripts are published online shortly after acceptance, before technical editing, formatting and proof reading. Using this free service, authors can make their results available to the community, in citable form, before we publish the edited article. This *Accepted Manuscript* will be replaced by the edited, formatted and paginated article as soon as this is available.

You can find more information about *Accepted Manuscripts* in the [Information for Authors](#).

Please note that technical editing may introduce minor changes to the text and/or graphics, which may alter content. The journal's standard [Terms & Conditions](#) and the [Ethical guidelines](#) still apply. In no event shall the Royal Society of Chemistry be held responsible for any errors or omissions in this *Accepted Manuscript* or any consequences arising from the use of any information it contains.



Cryptotanshinone inhibits proliferation and induces apoptosis via mitochondria-derived reactive oxygen species involving FOXO1 in the estrogen receptor-negative breast cancer Bcap37 cells

Received 00th January 20xx,
Accepted 00th January 20xx

DOI: 10.1039/x0xx00000x

www.rsc.org/

Xiaoman Liu^{a,b}, Lili Pan^a, Junling Liang^a, Jinhui Li^c, Shihua Wu^{*a}

Cryptotanshinone is a natural abietane type-diterpene quinone isolated from the lipophilic extract of Tanshen (or Danshen, *Salvia miltiorrhiza* Bunge) which was widely used in clinical application of treating inflammations such as acne, tonsillitis and mastitis in present days. Previous studies indicated that cryptotanshinone could not only inhibit the growth of androgen dependent and castration resistant prostate cancer cells by suppressing androgen receptor (AR), but also inhibit estrogen receptor (ER)-positive breast cancer cell proliferation by suppressing ER signals. In this work, we found cryptotanshinone can effectively inhibit the proliferation of ER-negative breast cancer Bcap37 cells. Cryptotanshinone induced a mitochondria-mediated apoptosis through changes in nuclear morphology, DNA fragmentation, loss of mitochondrial membrane potential, activation of caspase-like activities, and translocation of endonuclease G (EndoG) from mitochondria into nucleus. During the process, the caspases inhibitor could not completely abrogate apoptosis caused by cryptotanshinone, suggesting the intrinsic caspase-independent signaling functioned as one of the major pathways under high stress of cryptotanshinone. In addition, the apoptosis involved several key signals of cell proliferation and ROS regulation, such as suppression of PTEN and up-regulation of phosphorylated-AKT (Ser 473), thus the expression of a key transcription factor FOXO1 was down-regulated in further and resulted in accumulation of ROS that brought about the following oxidative DNA damage. In summary, the results showed that cryptotanshinone might be a promising apoptosis-induced agent in the treatment of ER-negative breast cancers by activation of mitochondria-derived ROS/FOXO1 signaling pathways.

1. Introduction

Although there are significant advancements in human health prevention and treatment, breast cancer is still the most frequently diagnosed cancer and is also the second worldwide leading cause of cancer death in females particularly in western countries^{1, 2}. During the past years, the receptor-targeting therapeutic strategies have been proved to be efficient to prolong survival for breast cancer patients with receptors of estrogen receptor (ER), progesterone receptor (PR), and or human epidermal growth factor receptor 2 (HER-2). ER was found to be a major receptor of breast cancer, and about 75% of breast cancers are ER- or PR-positive³⁻⁶. Thus, deprivation of estrogenic signaling pathways has been the main and key therapeutic form of hormonal therapy for patients with ER-positive and/or PR-positive diseases both pre- and postmenopausal patients⁷⁻⁹. However, definitive treatments of receptor-negative breast cancer including surgical resection, radiation, conventional chemotherapy, and

other systemic cures still face significant challenges owing to recurrence, acquired resistance and genomic instability of cancer cells. Therefore, breast cancer especially for ER-negative cancer and triple-negative breast cancer still takes a tremendous toll, and screening new and more effective prevention and chemotherapeutics are urgently needed.

Natural products have been used as one of the most important resources for new drug developments, especially for anti-cancer and anti-inflammatory drugs¹⁰⁻¹². In the course of screening new anti-cancer natural products, we found that tanshinones have potent cytotoxic activities for several cancer cells in vitro and thus prepared several high pure tanshinones from a famous Traditional Chinese Medicine Tanshen (or Danshen, *Salvia miltiorrhiza* Bunge) by use of unique liquid-liquid counter-current chromatography methods¹³⁻¹⁶. It has been known that tanshinones were the most prominent lipophilic diterpenoids¹⁷ and possesses potent pharmacological activities such as antibacterial, antioxidant, anti-inflammatory and antineoplastic^{18, 19}. Up to now, there are about 40 tanshinones isolated from the plant *S. miltiorrhiza* Bunge^{17, 19}.

Among the tanshinones, cryptotanshinone is one of the major constituents of the plant, previous studies indicated that cryptotanshinone has potent activities against several kinds of cancers. For example, cryptotanshinone may be used as a

^a Research Center of Siyuan Natural Pharmacy and Biotoxicology, College of Life Sciences, Zhejiang University, Hangzhou 310058, China.

^b School of Medicine, Shandong University, Jinan 250021, China.

^c Institute of Agrobiolgy and Environmental Sciences, Zhejiang University, Hangzhou 310058, China.

signal transducer and activator of transcription 3 (STAT3) inhibitor for suppressing proliferation and growth of prostate cancer^{20, 21}, human mucoepidermoid carcinoma²² and colorectal cancer²³, inducing endoplasmic reticulum stress-induced apoptosis in human hepatoma carcinoma HepG2²⁴ and human breast cancer MCF7 cells^{24, 25}. It is very interesting that cryptotanshinone could not only inhibit ER-positive breast cancer cell growth by suppressing estrogen receptor signaling²⁶, but also suppress androgen receptor-mediated growth in androgen dependent and castration resistant prostate cancer cells^{27, 28}. However, it is little known about its roles in the ER-negative breast cancer.

Therefore, the purpose of this work was to investigate the effects of cryptotanshinone in ER-negative breast cancer cells. Previous study indicated that human breast cancer Bcap37 cells are ER-negative²⁹. Thus we used this cell line to evaluate the role of cryptotanshinone. We found that cryptotanshinone not only inhibited proliferation and migration of Bcap37 cells, but also induced mitochondrial-mediated apoptosis. Furthermore, we found that the cell apoptosis induced by cryptotanshinone involved ROS production, FOXO1 inhibition and several relative PI3K/AKT/mTOR signals. Our findings show that cryptotanshinone may be an efficient candidate for ER-negative breast cancer via activation of mitochondria-derived ROS/FOXO1 pathways.

2. Materials and Methods

2.1. Materials

Cryptotanshinone (purity, more than 95%) was isolated and purified from the extracts of the root of *S. miltiorrhiza* Bunge by our gradient counter-current chromatography method¹⁵. Paclitaxel used as a positive contrast was purchased from National Institute for the Control of Pharmaceutical and Biological Products (NICBP) (Beijing, China). Compounds were all dissolved in dimethyl sulfoxide (DMSO) and stored in -20°C. 3-(4, 5-dimethyl-2-thiazolyl)-2, 5-diphenyl-2H-tetrazolium bromide (MTT) was purchased from Solarbio Science & Technology co., Ltd, Beijing, China. JC-1 Mitochondrial Membrane Potential Assay Kit was purchased from Cayman Chemical Company (CA, USA). Caspase inhibitor Z-VAD-FMK was purchased from Beyotime Biotechnology. BCA protein assay Kit was purchased from Thermo Electron Co. MA, USA. AnnexinV-FITC-PI apoptosis Kit was purchased from Biouniquer Technology Co., Ltd. Hoechst33342 was purchased from Invitrogen, CA, USA. ROS assay kit was purchased from Beyotime, China. Antibodies against ACTIN, PTEN, p-AKT(Ser 473), AKT, P-70S6K, p-P70S6K, FOXO1 and P27 were purchased from Cell Signalling Technology (Beverly, MA). Endo-G was purchased from SANTACRUZ Biotechnology Inc.

2.2. Cell culture

The human breast cancer cell line Bcap37 was cultured in RPMI 1640 medium (Gibco, USA) supplemented with 10% NBCS (v/v) (Gibco, USA), 2 mM-glutamine, penicillin (100 U/mL) and

streptomycin (100 U/mL) in humid condition of 37°C containing 5% CO₂.

2.3. Scratch motility (wound-healing) assay

Bcap37 cells were firstly seeded in a 24-well plate to the density of 90%, scratched for would lines with an 10 µL pipette tip, washed with PBS for twice and marked the would line on the plate. Then the cells were incubated with cryptotanshinone at the concentration of 0, 12.5 µM, 25 µM, and 50 µM for 24 h or 48 h. Each treatment was set for three repeats. Finally, cell motility was measured by counting number of the cells that migrated beyond the reference line³⁰.

2.4. Cell proliferation assay

Cell viability of Bcap37 cells was measured by MTT assay after treatment by tanshinones. Bcap37 cells (1×10⁴) growing in logarithmic phase were firstly seeded in 96-well plate for 24 h. Then the cells were treated with cryptotanshinone at the concentrations range from 10 to 50 µM at a final volume of 200 µL each well. After incubation for 48 h, the function of cryptotanshinone was terminated by adding 20 µL MTT solution (5 mg/mL) to each well and warmed in 37°C for 4 h. Finally, the produced formazan crystals were dissolved in 100 µL DMSO and tested in a microplate reader at the wavelength of 570 nm.

2.5. Apoptosis detection assays

2.5.1 AnnexinV-(fluorescein isothiocyanate) FITC/PI assay

Bcap37 cells treated by cryptotanshinone for 48 h were harvested, cell numbers were determined and quantified about 1×10⁶ cells in 1 mL of 1× binding buffer, then the cells were centrifuged at 1,500 rpm for 5 min. Supernatant was aspirated completely and cell pellets were resuspended in 250 µL of 1× binding buffer per 10⁶ cells. Then 5 µL AnnexinV-FITC was added per 10⁶ cells, mixed and incubated for 15 min in the dark at room temperature. Cells were washed by 1 mL of 1× binding buffer per 10⁶ cells and centrifuged at 1,500 rpm for 5 min. Supernatant was aspirated completely and cell pellets were resuspended in 250 µL of 1× binding buffer per 10⁶ cells. Then 5 µL PI solution was added immediately and stained for 5 min, finally the cells were analyzed by flow cytometry.

2.5.2 Nucleus morphology observation and DNA fragmentation assay

Bcap37 cells were treated by cryptotanshinone as in MTT assays. After 48 h, they were fixed in 75% ethanol for 15 min and stained with Hoechst33342 at the concentration of 5 µg/mL at 37°C for 15 min, finally the cells were captured under an Olympic inverted fluorescence microscope.

For DNA fragmentation assay, Bcap37 cells were seeded in a 6-well plate at the number of 1×10⁵ cells/well, after 24 h, they were treated with cryptotanshinone for 48 h, and harvested for genomic DNA extraction using the phenol/chloroform/isopentanol method and then their DNA were run in a 1.5% agarose gel for DNA ladders. Finally, the image of gel was captured under the gel imaging instrument.

2.6. Cell cycle analysis

The ultra-pure water and analytically pure ethanol were prepared in 4°C and -20°C beforehand. Bcap37 cells seeded in 6-well plate were harvested in tubes at 2,000 rpm for 5 min. The collected cells were suspended homogenizing distributed by 300 µL cold ultrapure water. Cell suspension was added to 700 µL pre-cold ethanol in each tube and mixed into uniform solution, kept in -20°C for about 12 h, washed in PBS for at least once, centrifuged at 2,000 rpm for 5 min. The cells were resuspended with 500 µL PI/RNase at a final concentration of 50 µg/mL for each tube, stained for at least 30 min and kept in 4°C protected from light. Finally, the samples were analyzed on flow cytometer for cell cycle analysis. The data was analyzed using the Modifit software for the analysis of cell cycle.

2.7. Mitochondrial membrane potential assay

Bcap37 cells were seeded in 96-well plate as before, after 24 h, they were treated with cryptotanshinone at the concentration of 3.125 µM, 6.25 µM, 12.5 µM, 25 µM and 50 µM for 48 h, each treatment for three repeats. Cells were stained in situ with JC-1 alive at a final concentration of 2 µM, each well for 50-100 µL in 37°C for about 30 min. Then they were washed with PBS for three times. Finally, the cells were imaged under an inverted fluorescence microscope.

2.8. ROS detection assay

Bcap37 cells were seeded in 24-well plate, after 24 h, they were treated with or without cryptotanshinone at the concentration of 12.5 µM, 25 µM and 50 µM for 48 h, each treatment for three repeats. Cells were washed with PBS and incubated with ROS probe in serum free medium alive for 30 min in 37°C according to the instruction of the kit. Then they were captured under an inverted fluorescence microscope at the wavelength of 488 nm. Additionally, Bcap37 cells were seeded on a 6-well plate and treated as above, harvested and incubated with ROS probes, the cells were analyzed on flow cytometry.

2.9. Immunofluorescent staining

Bcap37 cells treated with cryptotanshinone were firstly washed twice with ice-cold PBS and fixed in 4% PFA for 30 min at room temperature, then they were washed in PBS for three times again. After being blocked in 5% BSA in PBS/Triton for 30 min, the cells were incubated with primary antibody by diluting in PBS/Triton at 4°C overnight. Then the cells were rinsed three times in PBS for 5 min each, incubated with secondary antibody by diluting in PBS/Triton for 1 h in dark. At last, cells were stained with DAPI (5 µg/mL) in PBS for 5 min and washed three times in PBS for 5 min each. Finally, the cells were captured under a confocal laser scanning microscope (Zeiss, LSM710).

2.10. Western blot analysis

Proteins of cryptotanshinone treated Bcap37 cells for 48 h were harvested in lysis buffer on ice and centrifuged at 12,000 rpm for 5 min quickly. Supernatant was aspirated to another new tube, and quantified with BCA protein quantification kit (Thermo Scientific). The protein samples were loaded and run in SDS-PAGE gel, transformed to polyvinylidene fluoride (PVDF) membrane. The PVDF membrane was blocked in 5% non-fat milk for 1 h and incubated with primary antibody at 4°C overnight, washed in PBST for 3 times, 10 min each time. Then it was incubated with secondary antibody for 1 h, and washed in PBST for 3 times, 10 min for each time. After the reaction of ECL, films were developed in dark and scanned.

2.11. Statistical analysis

Data are expressed as means ± S.D. All experiments were repeated at least three times independently. Flow cytometry data of cell cycle were analyzed mainly by the software of Modifit. Figures of western blot were analyzed by the software of image J. In all cases, $p < 0.05$ was considered significant.

3. Results

3.1. Cryptotanshinone inhibits ER-negative breast cancer cell proliferation and migration

As shown in Fig. 1A, cryptotanshinone inhibited cell proliferation, induced cell shrinkage and condensed on morphology. Beside the widely effect on different kind of cell lines, MTT data (Fig. 1B and C) indicated that the inhibition effect of cryptotanshinone on Bcap37 cells were in dose- and time dependent manner.

Due to lack of estrogen receptor, Bcap37 cells showed stronger tendency of migration and invasion than other estrogen receptor positive breast cancers. Thus an *in vitro* wound healing assay³⁰ was used to measure the cell motility under the treatment of cryptotanshinone. Above MTT data indicated the cryptotanshinone was cytotoxic against Bcap37 cells at the high concentration. Thus a relative low concentration 12.5 µM was used to evaluate the effects on migration of breast cancer cells. As illustrated in Fig. 1D, cryptotanshinone showed significant inhibition activity on wound healing (migration) of Bcap37 cells at the low concentration of 12.5 µM for 24 h or 48 h.

3.2. Cryptotanshinone arrests cell cycle at S phase

Cell cycle is a key regulator of cell survival and repair signals network, it has direct effects on multiple cell processes, including cell proliferation, DNA repair, apoptosis and cell migration³¹. As described above, cryptotanshinone could inhibit cell proliferation and cell migration of Bcap37, thus cell cycle of Bcap37 was analyzed by flow cytometry. As shown in Fig. 2A, B, Bcap37 cells were reduced in G0/G1 phase, increased in S phase and showed no effect on G2/M phase, which indicated that the cells were arrested in S phase of mitosis cycle after treatment of different concentrations of cryptotanshinone for 48 h (Fig. 2B). Additionally, DNA in sub-

G1 showed a gradually raising tendency following the increase of the concentration of cryptotanshinone (Fig. 2A, C), which suggested that there was DNA fragmentation in Bcap37 cells and the cells might begin to die through cell apoptosis

pathway. This partially interpreted the inhibition on proliferation and migration of Bcap37 cells under the treatment of cryptotanshinone.

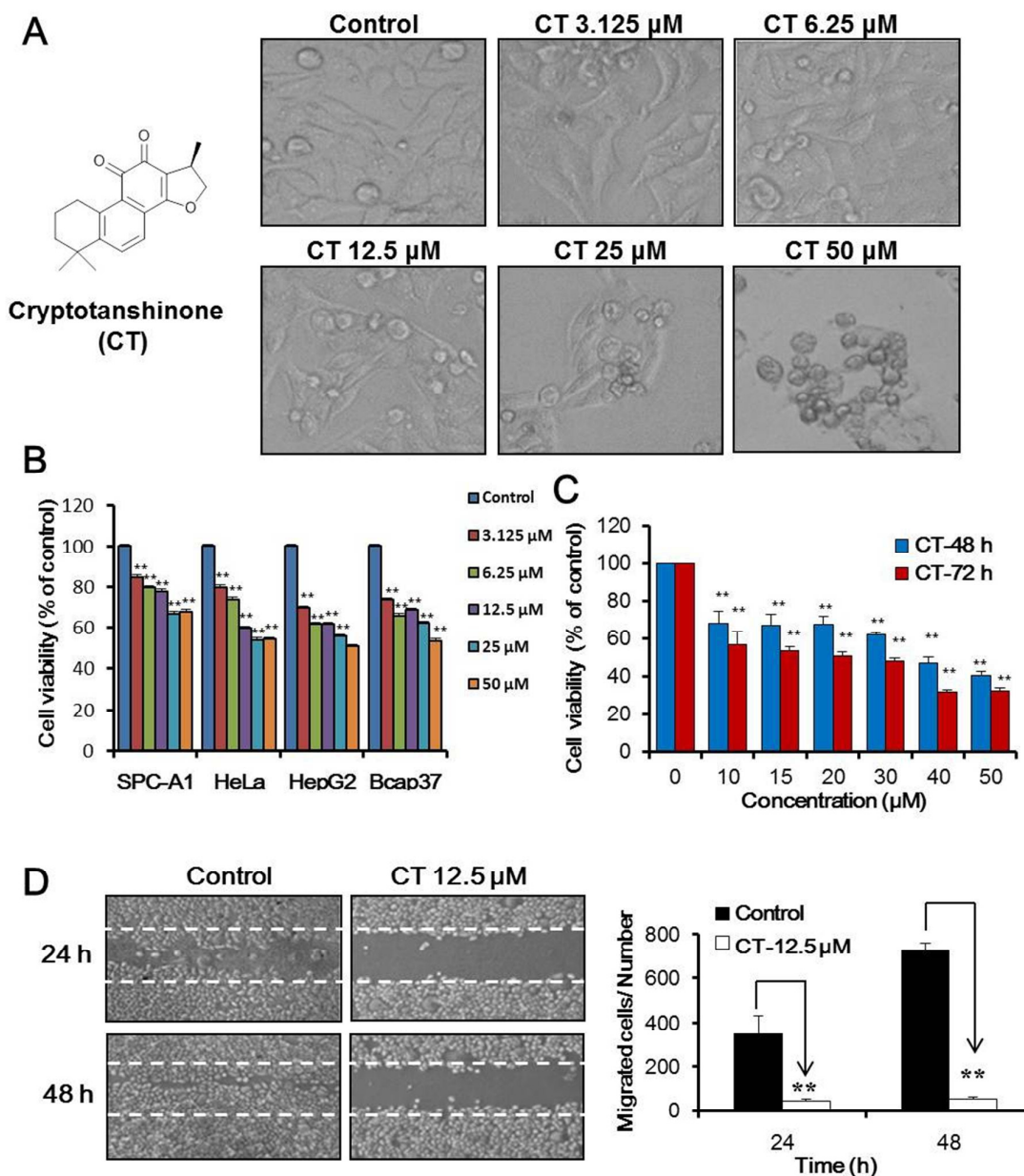


Fig. 1. Cryptotanshinone inhibited cell proliferation and migration of Bcap37 cells. (A) Left: Structures of cryptotanshinone (CT); Right: Bcap37 cells treated by CT at the concentrations of 3.125, 6.25, 12.5, 25 and 50 μM for 48 h. (B and C) Cell viability of Bcap37 cells treated by (B) CT at different concentrations from 10~50 μM for 48 h, (C) CT for different times of 48 h and 72 h, and the cell viability was tested by MTT method, each assay were repeated for at least 3 times. (D) Bcap37 cells were scratched with a 1 mm pipette, and treated with CT at the concentration of 12.5 μM . Left: optical microscopy pictures of Bcap37 cells were captured at 24 h and 48 h. Right: Statistic of the migrated cells after treated with CT at the concentration of 12.5 μM for 24 h and 48 h. Results are expressed as the mean \pm SE * p < 0.05, ** p < 0.01 compared with control.

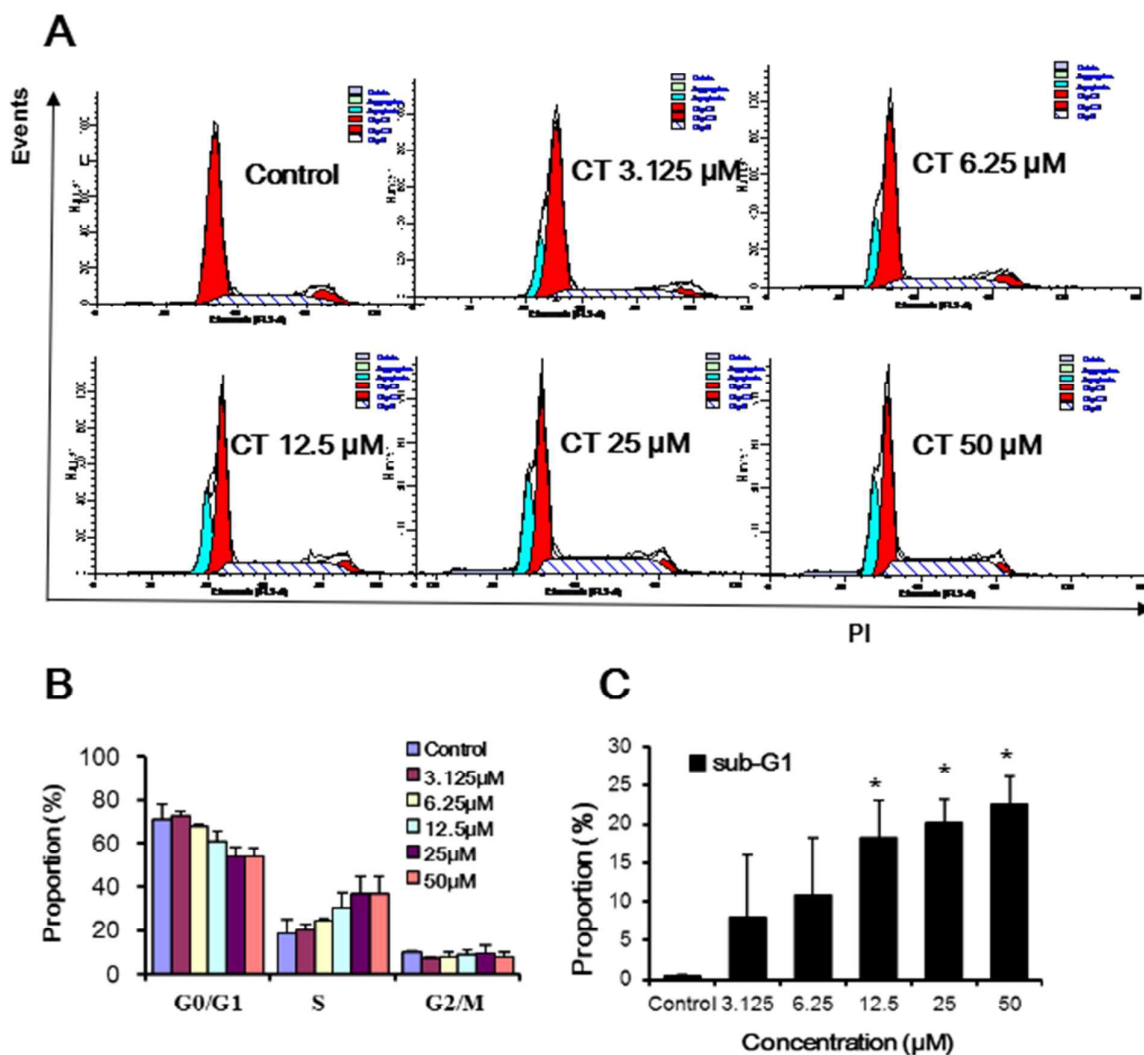


Fig. 2. Cryptotanshinone induced cell cycle arrest in S phase and the increase of DNA into sub-G1 phase. (A) Typical images of cell cycle assay at the indicated concentrations. Cells were treated as above at 3.125, 6.25, 12.5, 25 and 50 μM for 48 h, stained with PI (50 $\mu\text{g}/\text{mL}$) for 30 min, and finally analyzed by flow cytometry, the assay was repeated for three times and analyzed through the software of Modifit. (B and C) Proportion of cells in G0/G1, S and G2/M phases (B), and that were induced apoptosis in Bcap37 cells treated by different concentrations of CT (C). The results are expressed as the mean \pm SE (* $p < 0.05$).

3.3. Cryptotanshinone induced dose and time-dependent cell apoptosis

To clarify the formation of the DNA in sub-G1, the nuclear morphology of Bcap37 cells treated by cryptotanshinone was monitored. The results (Fig. 3A, B) indicated that there were an increasing number of nuclear condensed and fragmented

cells with the concentration increase of cryptotanshinone. As is well known, one of the biochemical markers of apoptosis is DNA fragmentation into different fragments of 180 bp units³². Thus the genomic DNA of Bcap37 cells was extracted and the DNA ladder assay was performed.

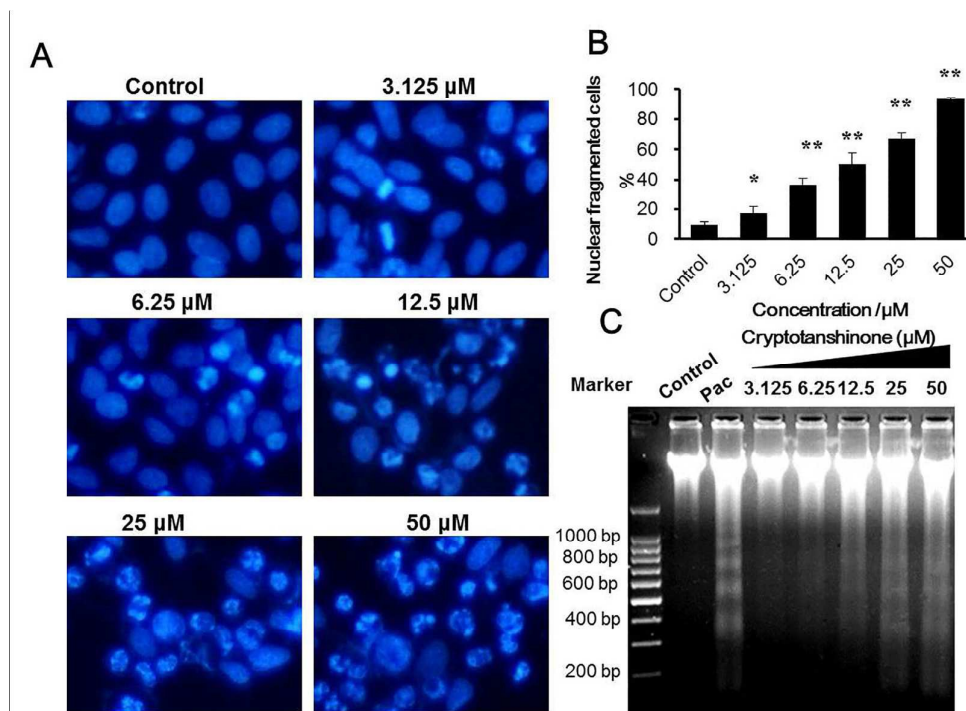


Fig. 3. Cryptotanshinone induced fragmentation of cell nucleus and produced DNA ladders. (A) Bcap37 cells treated with different concentrations for 48 h, were stained with Hoechst33342 and were captured under an inverted fluorescent microscope. (B) Statistic of the proportion of cells with fragmented nuclei after cryptotanshinone treated for 48 h. * $P < 0.05$, statistically significant in comparison with control. (C) Cells treated with cryptotanshinone in different concentrations range from 3.125 to 50 μM and paclitaxel (Pac) at 2.34 μM as a positive control for 48h. Cell DNA was extracted and run on a 1.5 % agarose gel for the DNA ladders. "Con" indicated control without medicine treatment. The assay was repeated for three times. The results are expressed as the mean \pm SE (* $p < 0.05$, ** $p < 0.01$).

As shown in Fig. 3C, there was significant amount of DNA fragments at 180, 360, 540 and 720 bp in Bcap37 cells treated by cryptotanshinone for 48 h at different concentrations from 3.125-50 μM . It was closely in agreement with the result of the increasing sub-G1 DNA detected from the cell cycle assay in cryptotanshinone treated Bcap37 cells at the concentration of 3.125-50 μM (Fig. 2C).

In addition, the cells treated by cryptotanshinone were analyzed by AnnexinV-FITC/PI assay on flow cytometry. The results (Fig. 4) indicated that cryptotanshinone induced the early apoptosis of Bcap37 cells in a dose- (Fig. 4A, B) and time- (Fig. 4C, D) dependent manner. When the Bcap37 cells were treated at the concentration of 25 μM for 48 h, a proportion of about 18% were induced to be early apoptotic cells. To explore the involved apoptotic pathway in Bcap37 cells, the optimum concentration of cryptotanshinone at 25 μM was selected for the following assays.

3.4. Cryptotanshinone decreased mitochondrial membrane potential

Since mitochondria are cellular organelles that are sensitive to apoptosis, we applied the mitochondria membrane potential detecting fluorescence probe JC1 in this case. As shown in Fig. 5 A and B, it was apparent that mitochondria membrane potential was gradually decreased with the increase of the concentration of cryptotanshinone from 6.25 μM to 50 μM . Typically, the mitochondria membrane potential of cells showed distinct decrease by 20% to 60 % under the concentration of cryptotanshinone from 12.5 μM to 50 μM compared with the intensity in control cells. This implied that cryptotanshinone induced Bcap37 cells apoptosis through mitochondria dependent intrinsic pathway.

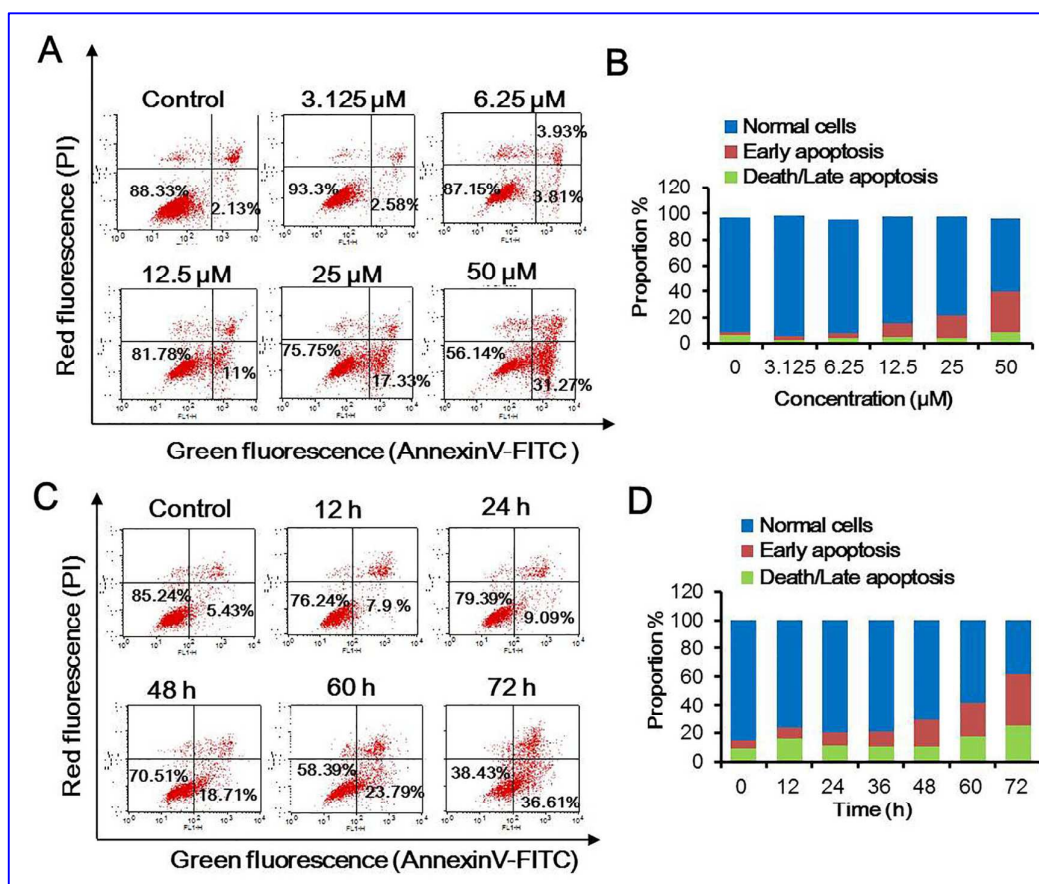


Fig. 4. Cryptotanshinone induced dose and time-dependent apoptosis of Bcap37 cells. (A) Flow cytometry data of Bcap37 cells treated with cryptotanshinone at the concentration of 0, 3.125, 6.25, 12.5, 25 and 50 μM for 48 h, stained with AnnexinV-FITC/PI. (C) Flow cytometry data of Bcap37 cells treated with cryptotanshinone at 25 μM in different times of 12, 24, 48, 60, 72 h. (B and D) Column diagram of the data in (A and C) analyzed by the software ModiFit.

3.5. Cryptotanshinone induced caspase-dependent and independent apoptosis in Bcap37 cells

In most of the cases, cell apoptosis mainly involved activation of several caspases including caspase initiators and caspase executioners³³. As shown in Fig. 5 C, Bcap37 cells treated by cryptotanshinone for 48 h showed apparent nuclear fragmentations and the increased expression of cleaved caspase-3 which is an active form of caspase executioner cleaved from caspase-3. Thus the result indicated that the apoptosis induced by cryptotanshinone underwent a caspase-dependent process. To confirm this, we measured cell apoptosis after the pre-treatment with or without caspase inhibitors for 2 h before co-culturing Bcap37 cells with cryptotanshinone. However, we found that the apoptosis was only slightly rescued when treated with cryptotanshinone together with the caspase inhibitor (Z-DEVD-fmk) in Bcap37 cells, compared with cryptotanshinone only treated cells (Fig 5D, E). It implied that a caspase-independent pathway might also be involved in the cryptotanshinone-induced cell death. Besides caspase-dependent apoptosis, cell death also goes in the caspase-independent ways³³ by activating several signals

such as apoptosis-inducing factor (AIF)³⁴ and nuclear encoded protein endonuclease G (EndoG)³⁵. As is well known, EndoG is a mitochondria protein that can lead to DNA fragmentation directly and represents a caspase-independent pathway in cell apoptosis³⁵. In our case, the mitochondrial protein EndoG was shown to gradually translocate from mitochondria to nucleus according to the progress of cell apoptosis (Fig. 5 F). Additionally, we quantified the expression of EndoG at the protein level and found that the expression level of EndoG was up-regulated especially under the treatment of high concentration of 12.5 and 25 μM of cryptotanshinone (Fig. 5G).

3.6. Cryptotanshinone induced apoptosis involved ROS production, FOXO1 inhibition and PI3K/AKT signalling pathways

Recently, reactive oxygen species (ROS)-targeting strategy has been thought to be a promising radical therapeutic approach for cancer cells. Chemically, ROS is a collective term that describes the chemical species that are formed upon incomplete reduction of oxygen and includes the superoxide

anion (O_2^-), hydrogen peroxide (H_2O_2) and the hydroxyl radical (HO^\bullet)³⁶.

A moderate increase in ROS can promote cell proliferation, cell differentiation and protect cells from apoptosis, whereas excessive amounts of ROS can bring about oxidative damage to lipids, protein and DNA³⁷, the disruption of the mitochondria membrane potential and the release of cytochrome C by oxidation of mitochondrial pores, which subsequently induces cell apoptotic death^{38,39}. There are numbers of anti-cancer compounds that were found to induce cell death through ROS-mediated mechanism. For example, accumulation of hydrogen peroxide is an early and crucial step for paclitaxel-induced cancer cell death both in vitro and in vivo⁴⁰.

However, cancer cells can express much more antioxidants such as FOXO1 to resist the cytotoxic stress⁴¹. FOXO1 protein is one of the transcription factors that are implicated in cell cycle, DNA damage, cell proliferation and apoptosis. Oxidative stress could induce nuclear translocation of FOXO proteins, thus FOXO proteins could induce expressions of genes involved in oxidative stress resistance, cell cycle arrest and apoptosis³¹⁻³³. Screening some new ROS generators with lower antioxidant levels such as arsenic trioxide (As_2O_3)⁴² and the natural product piperlongumine⁴³ are still very important for current drug development.

In this case, ROS production in Bcap37 cells was highly increased in a concentration dependent way (Fig. 6), which was in accordance with the known results that cryptotanshinone induced apoptosis in other tumor cells such as rhabdomyosarcoma (Rh30), prostate carcinoma (DU145) and HepG2 cells⁴⁴⁻⁴⁶.

It has been known that ROS can also act as second messengers regulating cell signaling pathways and also induce cell apoptosis or senescence when it is accumulated at high level^{47,48}. In our works, the PI3K/AKT pathway was found to be activated by treatment of cryptotanshinone. In addition, the tumor suppressor PTEN was also inhibited, which directly led to the increase of the p-AKT (Ser473) even at the low concentration of 6.25 μ M.

The downstream transcription factor FOXO1, an antioxidant player and an inhibitor of cell apoptosis^{48,49}, was responsively decreased in Bcap37 cells. Additionally, phosphorylation of the substrate (P-P70S6K) of mTOR pathway was found to be increased (Fig. 7A), which contributed to the high level of ROS.

4. Discussion

Diterpenoid tanshinones have attracted particular attention from medicinal chemists and clinicians, because tanshinones possess a variety of pharmacological activities such as antibacterial, antioxidant, anti-inflammatory, and antineoplastic¹⁹. Besides three tanshinones including tanshinone IIA, tanshinone I, and cryptotanshinone as the major constituents of the plant, there are total 40 tanshinones to be isolated from the plant^{17,19}. Among the tanshinones,

cryptotanshinone has been found to be more efficient or sensible to several human cancer cells than other tanshinones.

In the present study, we found that cryptotanshinone could inhibit ER-negative breast cancer Bcap37 cells proliferation and migration (Fig. 1) and induce shrinkage on cell morphology (Fig. 1A), cell cycle arrest in S phase and sub-G1 (Fig. 2). Apoptosis, or programmed cell death, is central to the development and homeostasis of metazoans^{33,50}. The morphological changes of apoptosis include membrane blebbing, cell shrinkage, chromatin condensation, and formation of apoptotic bodies⁵¹. We observed these characteristics of apoptotic morphological changes including nuclear condensation or fragmentation and DNA fragmentation after cryptotanshinone treatment in Bcap37 cells (Fig. 3). Annexin V/PI assay which allows us to quantify the apoptotic cells, showed that cryptotanshinone induced early apoptosis on Bcap37 cells in a dose- and time-dependent way (Fig. 4).

Mitochondria play key roles in activating apoptosis in mammalian cells⁵². We found that there was a significant decrease of mitochondrial membrane potential in Bcap37 cells induced by cryptotanshinone (Fig. 5A and B). Then it was also found that the active apoptotic protein cleaved-caspase 3 highly expressed especially in the nuclear-fragmented cells induced by cryptotanshinone (Fig. 5C, D). This suggested that cryptotanshinone induced a caspase-mediated apoptosis.

However, caspases inhibitor could not arrest completely the cryptotanshinone-induced apoptosis (Fig. 5D and E). This implied that there was a caspase-independent apoptotic pathway. There are several signals involving the activation of caspase-independent apoptosis process, such as AIF and EndoG^{34,35}. Here we found the protein EndoG gradually translocated to nucleus (Fig. 5F) and highly expressed especially under high stress of cryptotanshinone (Fig. 5G). In this case, EndoG released independent of the activation of caspases. It indicated that cryptotanshinone might meanwhile trigger the caspase-independent apoptotic pathway together with caspase-dependent apoptotic pathway when under high concentration of cryptotanshinone in Bcap37 cells.

ROS is one of the most important signals triggering apoptosis⁴⁸. As shown in Fig. 6, cryptotanshinone induce high level of ROS in a concentration dependent way in Bcap37 cells. It has been known that mitochondria is the source and also the target of ROS, while excessive ROS might disrupt mitochondria membrane potential^{48,53} and induce apoptosis^{48,54}. In this case, Bcap37 cells showed low mitochondrial membrane potential and fell in caspase-independent and dependent apoptosis under high level of ROS (Fig. 5)⁴⁹.

ROS is also an important second messenger to activate a series of cell signalling pathways such as ERK pathway, SAPK pathways, PKC pathway and PI3K/AKT pathway, and so on^{50,55,56}. In the current study, the PI3K/AKT pathway (Fig. 7) was found activated by cryptotanshinone and the downstream signals were correspondingly regulated.

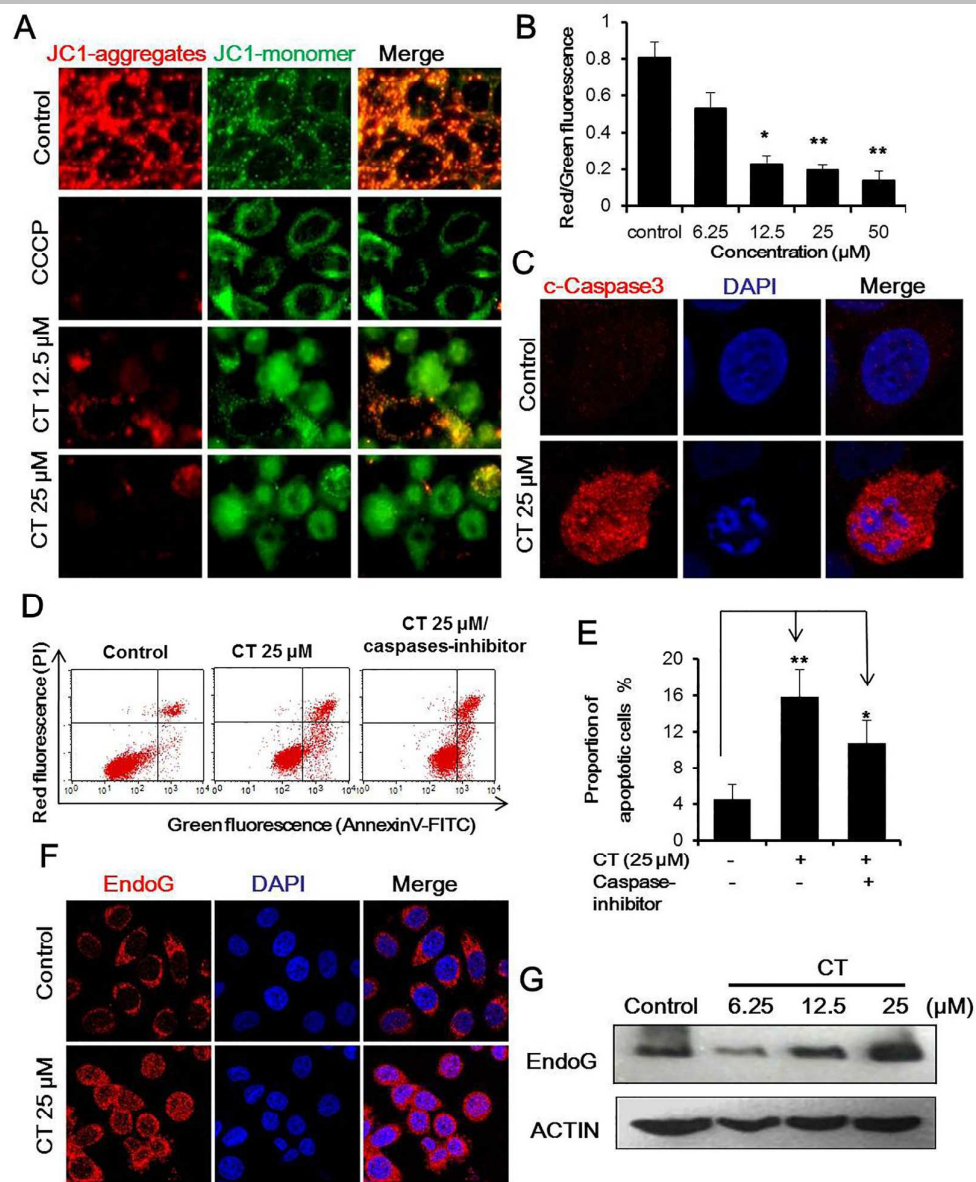


Fig. 5. Cryptotanshinone (CT) induced Bcap37 cells apoptosis through a caspase-dependent and independent pathway. (A) Fluorescence images of typical Bcap37 cells with JC-1 staining after cryptotanshinone (CT) treated for 48 h. (B) Mitochondria membrane potential change of Bcap37 cells treated by different concentrations of CT. The data was analyzed through the software of image J from the figures captured in (A). (C) Fluorescence images of typical Bcap37 cells immuno-stained with antibodies of cleaved-Caspase-3. (D) Flow cytometry data of Bcap37 cells treated by CT at the concentration of 25 μM with or without caspase inhibitors for 48 h with AnnexinV-FITC/PI staining. (E) Statistics for result of data from (D). (F) Fluorescence images of Bcap37 cells stained with EndoG antibody. (G) Expression of EndoG in Bcap37 cells treated by CT for 48 h through western blot. The results are expressed as the mean \pm SE (* p < 0.05, ** p < 0.01).

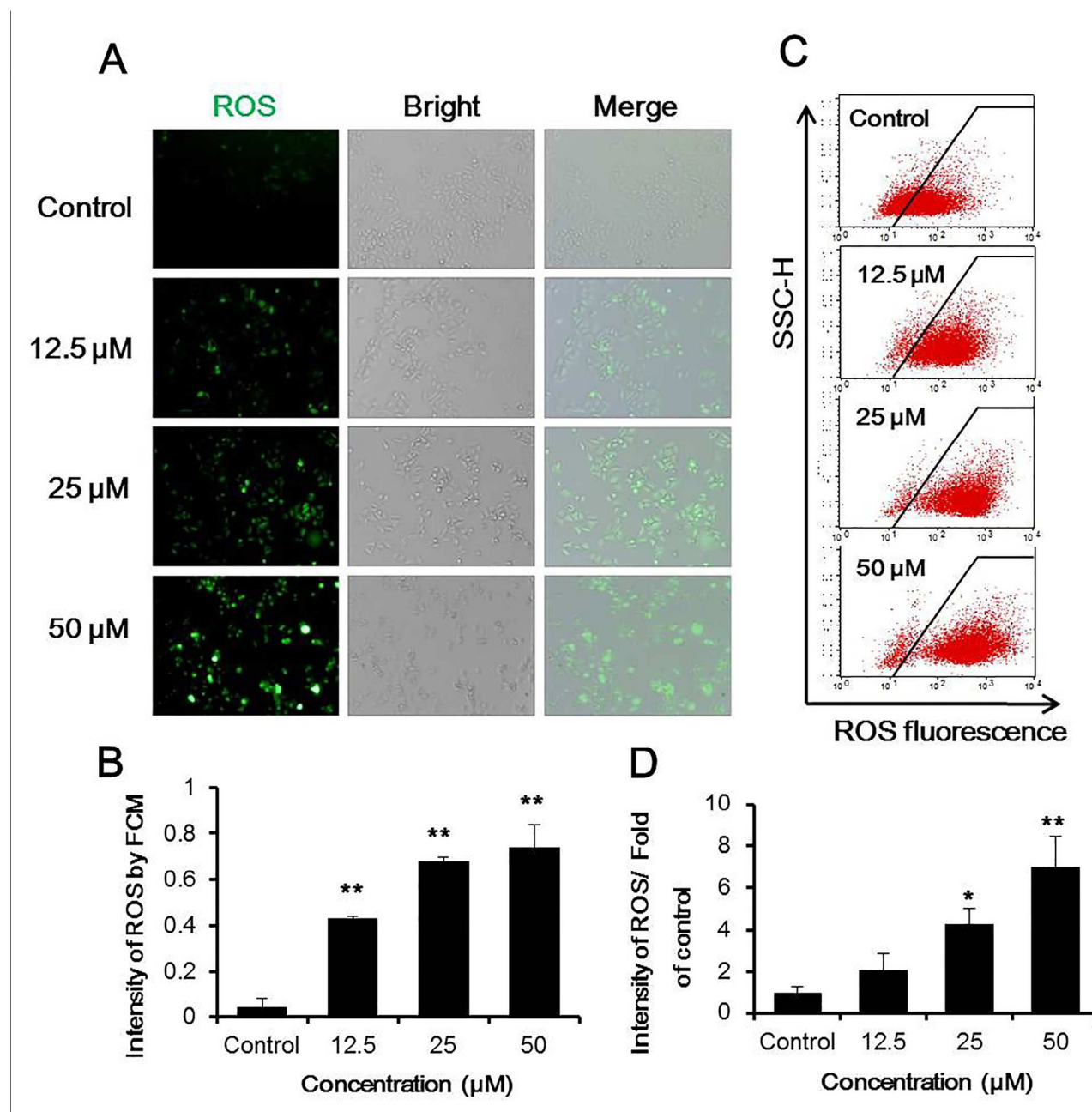


Fig. 6. Cryptotanshinone induce ROS accumulation in a concentration dependent way. (A) Fluorescence images of Bcap37 cells treated with cryptotanshinone and stained with the molecular probe DCFH-DA of ROS. (B) Proportion of cells with ROS positive signals in figure (A). (C) Flow cytometry analysis of cells stained by the molecular probe DCFH-DA of ROS. (D) Statistic of cell intensity of ROS signals tested by flow cytometry at different concentrations in (C). The results are expressed as the mean \pm SE (* p < 0.05, ** p < 0.01).

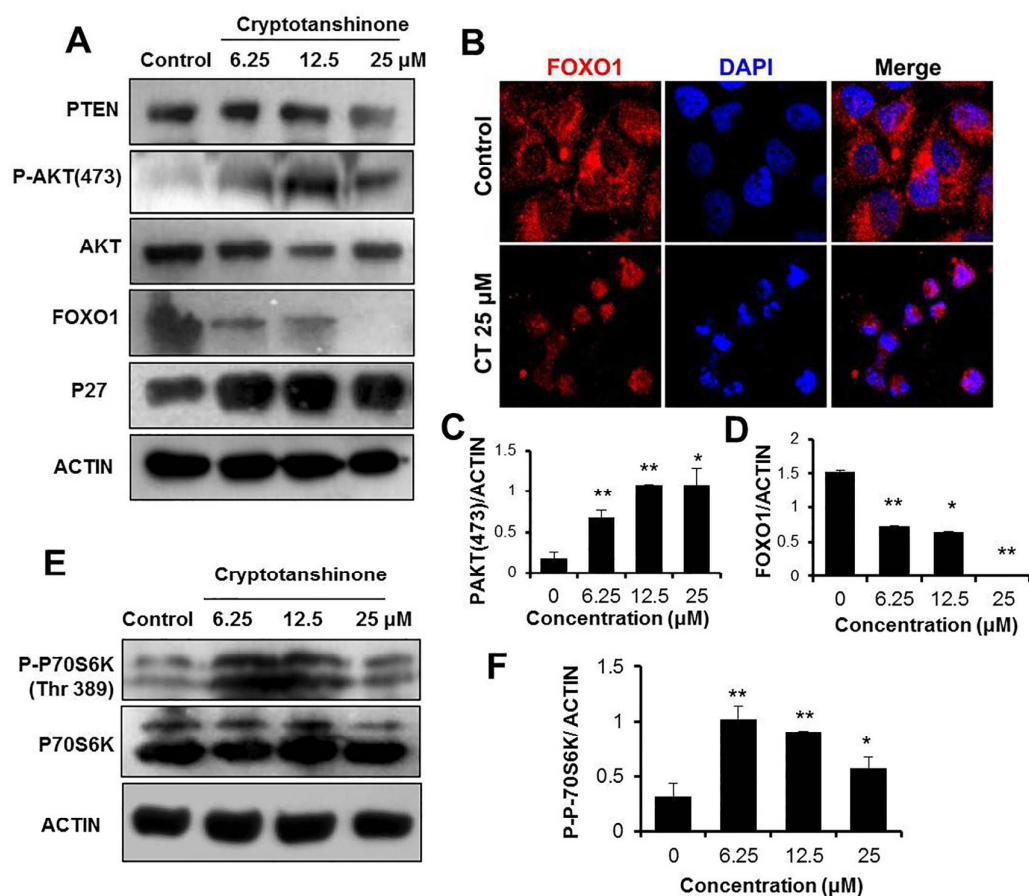


Fig. 7. Cryptotanshinone activated PI3K/AKT/mTOR pathway. (A), Proteins of PI3K/AKT signaling pathway in cryptotanshinone treated Bcap37 cells were detected by western blot. (B, C and D) The proportions of expressions of p-P-70S6K, p-AKT (473) and FOXO1 in Bcap37 cells treated by different concentrations of cryptotanshinone for 48 h, the data was analyzed by the software of image J. The results are expressed as the mean \pm SE (* p < 0.05, ** p < 0.01).

FOXO1 is a transcriptional factor and acts as an antioxidant which can inhibit the production of ROS⁵⁷. Previous study⁵⁸ indicated that FOXO1 may promote wound healing and prevention of oxidative stress. In this work, FOXO1 was inhibited evidently, resulting in increasing ROS accumulation (Fig. 6) and the inhibition of wound healing (Fig. 1D). In addition, one of the substrates of mTOR pathway phosphorylated-P70S6K was also activated. Additionally,

activation of the PI-3K/AKT pathway and the nucleus translocation of FOXO1 from the cytoplasm might increase the level of the key cell division regulator P27, which contributed to arrest of cell cycle at S phase in Bcap37 cells and was responsible for cell proliferation inhibition⁵⁹. Therefore, cryptotanshinone induced cell apoptosis, inhibited cell proliferation and cell migration through ROS mediated PI3K/AKT/mTOR pathway in breast cancer Bcap37.

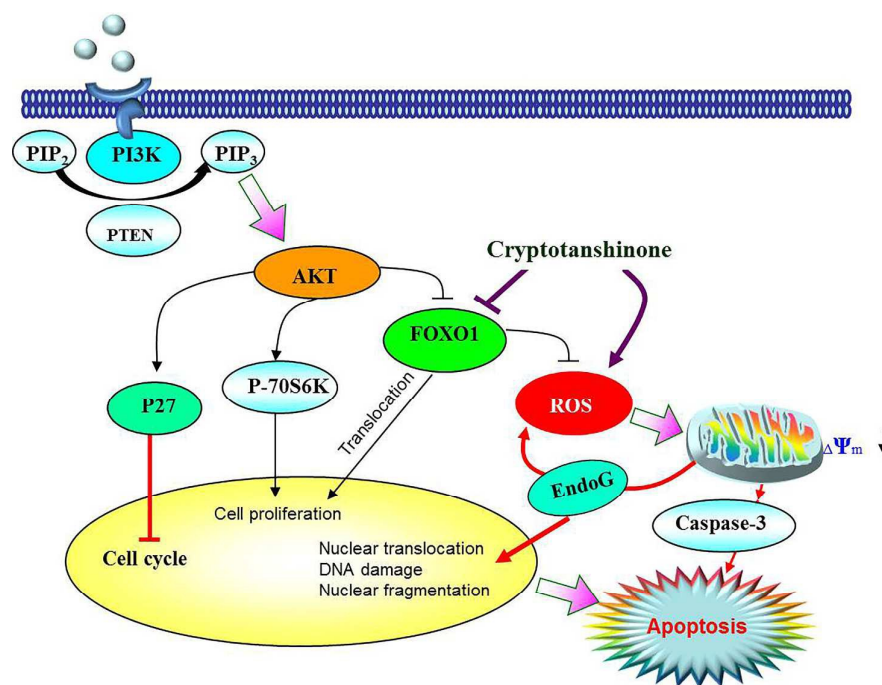


Fig. 8. The proposed molecular signaling network pathways involved in cryptotanshinone induced apoptosis and cell growth inhibition. Two key transcription factors of FOXO1 and ROS molecules were found to be involved in cryptotanshinone induced signals. On the one hand, cryptotanshinone down-regulated the expression of FOXO1 and resulted in the ROS accumulation and following oxidative DNA damage, resulted in apoptosis. On the other hand, cryptotanshinone increased the cell cycle regulation protein P27 and led to the arrest of cell proliferation and migration.

5. Conclusions

In summary, as proposed in Fig. 8, this work provided new clues to understand the mechanism of cryptotanshinone induced apoptosis on ER-negative breast cancers. Although it still need do many works to know its mechanism *in vivo* in future, our present study demonstrated that cryptotanshinone was an efficient ROS generator *in vitro*, and could inhibit cell proliferation and migration, induce apoptotic cell death in the ER-negative breast cancer cells Bcap37 by inhibiting the antioxidant FOXO1 through the activation of the PI3K/AKT/mTOR signaling pathway. Thus, cryptotanshinone might be a promising candidate in the treatment of ER-negative breast cancers by inducing apoptosis and inhibiting cell migration through the ROS-mediated PI3K/AKT/mTOR pathways. To the best of our knowledge, this is the first report to demonstrate the potential anti-cancer efficiency of cryptotanshinone on ER-negative breast cancer through the ROS-mediated PI3K/AKT/mTOR signalling pathways.

Acknowledgements

The authors apologize to colleges whose work could not be cited owing to lack of space. This work was supported in part by the National Natural Science Foundation of China (Grant No. 20972136, 21272209).

References

- 1 R. Siegel, E. Ward, O. Brawley and A. Jemal, *CA Cancer J. Clin.*, 2011, **61**, 212-236.
- 2 R. Siegel, D. Naishadham and A. Jemal, *CA Cancer J. Clin.*, 2013, **63**, 11-30.
- 3 A. Brodie and G. Sabnis, *Clin. Cancer Res.*, 2011, **17**, 4208-4213.
- 4 E. R. Simpson, *J. Ster. Biochem. Mol. Biol.*, 2003, **86**, 225-230.
- 5 J. D. Yager and N. E. Davidson, *New Engl. J. Med.*, 2006, **354**, 270-282.
- 6 Y. Tsuchiya, M. Nakajima and T. Yokoi, *Cancer Lett.*, 2005, **227**, 115-124.
- 7 I. E. Smith and M. Dowsett, *New Engl. J. Med.*, 2003, **348**, 2431-2442.
- 8 S.-X. Lin, J. Chen, M. Mazumdar, D. Poirier, C. Wang, A. Azzi and M. Zhou, *Nat. Rev. Endocrinol.*, 2010, **6**, 485-493.
- 9 A. Howell and M. Dowsett, *Brit. Med. J.*, 1997, **315**, 863-866.
- 10 J. N. a. G. M. Cragg, *J. Nat. Prod.*, 2012, **75**, 311-335.
- 11 J. W. H. L. a. J. C. Vederas, *Science*, 2009, **325**, 161-165.
- 12 F. E. K. a. G. T. Carter, *Nat Rev Drug Discov.*, 2005, **4**, 206-220.
- 13 J. Meng, Z. Yang, J. Liang, H. Zhou and S. Wu, *J. Chromatogr. A*, 2014, **1323**, 73-81.
- 14 J. Meng, Z. Yang, J. Liang, M. Guo and S. Wu, *J. Chromatogr. A*, 2014, **1327**, 27-38.
- 15 S. Wu, D. Wu, J. Liang and A. Berthod, *J. Sep. Sci.*, 2012, **35**, 964-976.
- 16 D. Wu, X. Jiang and S. Wu, *J. Sep. Sci.*, 2010, **33**, 67-73.
- 17 Y. G. Li, L. Song, M. Liu, H. Zhi Bi and Z. T. Wang, *J. Chromatogr. A*, 2009, **1216**, 1941-1953.
- 18 L. M. Zhou, Z. Zuo and M. S. S. Chow, *J. Clin. Pharmacol.*, 2005, **45**, 1345-1359.
- 19 X. H. Wang, S. L. Morris-Natschke and K. H. Lee, *Med. Res. Rev.*, 2007, **27**, 133-148.
- 20 D. S. Shin, H. N. Kim, K. D. Shin, Y. J. Yoon, S.-J. Kim, D. C. Han and B.-M. Kwon, *Cancer Res.*, 2009, **69**, 193-202.
- 21 K. Sung-Hoon, *Korean J. Orient. Physiol. Pathol.*, 2012, **26**, 437-440.
- 22 H. J. Yu, C. Park, S.-J. Kim, N. P. Cho and S. D. Cho, *Pharmacognosy Mag.*, 2014, **10**, 622-629.
- 23 W. Li, S. M. Saud, M. R. Young, N. H. Colburn and B. Hua, *Mol. Cell. Biochem.*, 2015, **406**, 63-73.
- 24 I. J. Park, M. J. Kim, O. J. Park, W. Choe, I. Kang, S. S. Kim and J. Ha, *Apoptosis*, 2012, **17**, 248-257.
- 25 Y. F. Zhang, M. Zhang, X. L. Huang, Y. J. Fu, Y. H. Jiang, L. L. Bao, Y. M. Maimaitiying, G. J. Zhang, Q. Q. Wang and H. Naranmandura, *Metallomics*, 2015, **7**, 165-173.
- 26 S. Li, H. Wang, L. Hong, W. Liu, F. Huang, J. Wang, P. Wang, X. Zhang and J. Zhou, *Cancer Biol. Ther.*, 2015, **16**, 176-184.

Journal Name ARTICLE

- 27 D. Xu, T.-H. Lin, S. Li, J. Da, X.-Q. Wen, J. Ding, C. Chang and S. Yeh, *Cancer Lett.*, 2012, **316**, 11-22.
- 28 Y. Zhang, S.-H. Won, C. Jiang, H.-J. Lee, S.-J. Jeong, E.-O. Lee, J. Zhang, M. Ye, S.-H. Kim and J. Lu, *Pharmaceut. Res.*, 2012, **29**, 1595-1608.
- 29 M. Sui, Y. Huang, B. H. Park, N. E. Davidson and W. Fan, *Cancer Res.*, 2007, **67**, 5337-5344.
- 30 L. G. Rodriguez, X. Wu and J.-L. Guan, *Methods in mol. biol. (Clifton, N.J.)*, 2005, **294**, 23-29.
- 31 M. Boehm and E. G. Nabel, *Circulation*, 2001, **103**, 2879-2881.
- 32 A. H. Wyllie, J. F. Kerr and A. R. Currie, *Int. review cytol.*, 1980, **68**, 251-306.
- 33 S. J. Riedl and Y. Shi, *Nat. Rev. Mol. Cell Biol.*, 2004, **5**, 897-907.
- 34 L. Yang, X. Liu, Z. Lu, J. Y.-W. Chan, L. Zhou, K.-P. Fung, P. Wu and S. Wu, *Cancer Lett.*, 2010, **298**, 128-138.
- 35 L. Y. Li, X. Luo and X. Wang, *Nature*, 2001, **412**, 95-99.
- 36 B. D'Autreaux and M. B. Toledano, *Nat. Rev. Mol. Cell Biol.*, 2007, **8**, 813-824.
- 37 D. Trachootham, J. Alexandre and P. Huang, *Nat. Rev. Drug Discov*, 2009, **8**, 579-591.
- 38 J. Watson, *Open Biol.*, 2013, **3**, 120144.
- 39 C. Wang and R. J. Youle, *Annu. Rev. Genet.*, 2009, **43**, 95-118.
- 40 J. Alexandre, F. Batteux, C. Nicco, C. Chereau, A. Laurent, L. Guillevin, B. Weill and F. Goldwasser, *Int. J. Cancer*, 2006, **119**, 41-48.
- 41 T. Goto, M. Takano, J. Hirata and H. Tsuda, *Brit. J. Cancer*, 2008, **98**, 1068-1075.
- 42 J. Lu, E.-H. Chew and A. Holmgren, *Proc. Nat. Acad. Sci. USA*, 2007, **104**, 12288-12293.
- 43 L. Raj, T. Ide, A. U. Gurkar, M. Foley, M. Schenone, X. Li, N. J. Tolliday, T. R. Golub, S. A. Carr, A. F. Shamji, A. M. Stern, A. Mandinova, S. L. Schreiber and S. W. Lee, *Nature*, 2011, **475**, 231-234.
- 44 W. Y. W. Lee, K. W. K. Liu and J. H. K. Yeung, *Cancer Lett.*, 2009, **285**, 46-57.
- 45 I.-J. Park, M.-J. Kim, O. J. Park, M. G. Park, W. Choe, I. Kang, S.-S. Kim and J. Ha, *Cancer Lett.*, 2010, **298**, 88-98.
- 46 W. Chen, L. Liu, Y. Luo, Y. Odaka, S. Awate, H. Zhou, T. Shen, S. Zheng, Y. Lu and S. Huang, *Cancer Prevent. Res.*, 2012, **5**, 778-787.
- 47 J. E. Le Belle, N. M. Orozco, A. A. Paucar, J. P. Saxe, J. Mottahedeh, A. D. Pyle, H. Wu and H. I. Kornblum, *Cell Stem Cell*, 2011, **8**, 59-71.
- 48 H. U. Simon, A. Haj-Yehia and F. Levi-Schaffer, *Apoptosis*, 2000, **5**, 415-418.
- 49 V. J. Thannickal and B. L. Fanburg, *Amer. J. Physiol. Lung Cell. Mol. Physiol.*, 2000, **279**, L1005-L1028.
- 50 P. D. Ray, B.-W. Huang and Y. Tsuji, *Cell. Signal.*, 2012, **24**, 981-990.
- 51 S. Rello, J. C. Stockert, V. Moreno, A. Gamez, M. Pacheco, A. Juarraz, M. Canete and A. Villanueva, *Apoptosis*, 2005, **10**, 201-208.
- 52 D. R. Green and J. C. Reed, *Science*, 1998, **281**, 1309-1312.
- 53 G.-Y. Li, K. H. Jung, H. Lee, M. K. Son, J. Seo, S.-W. Hong, Y. Jeong, S. Hong and S.-S. Hong, *Cancer Lett.*, 2013, **329**, 59-67.
- 54 S. Rakshit, L. Mandal, B. C. Pal, J. Bagchi, N. Biswas, J. Chaudhuri, A. A. Chowdhury, A. Manna, U. Chaudhuri, A. Konar, T. Mukherjee, P. Jaisankar and S. Bandyopadhyay, *Biochem. J. Pharmacol.*, 2010, **80**, 1662-1675.
- 55 M. Zamkova, N. Khromova, B. P. Kopnin and P. Kopnin, *Cell Cycle*, 2013, **12**, 826-836.
- 56 J. L. Martindale and N. J. Holbrook, *J. Cell. Physiol.*, 2002, **192**, 1-15.
- 57 Y. Akasaki, O. Alvarez-Garcia, M. Saito, B. Carames, Y. Iwamoto and M. K. Lotz, *Arthritis Rheumatol*, 2014, **66**, 3349-3358.
- 58 B. Ponugoti, F. Xu, C. Zhang, C. Tian, S. Pacios and D. T. Graves, *J. cell biol.*, 2013, **203**, 327-343.
- 59 M. B. Moller, *Leuk Lymphoma*, 2000, **39**, 19-27.

